

## Inversion in the change of the refractive index and memory effect near the nematic-isotropic phase transition in a lyotropic liquid crystal

J. R. D. Pereira,<sup>1,2</sup> A. J. Palangana,<sup>1</sup> A. M. Mansanares,<sup>2</sup> E. C. da Silva,<sup>2</sup> A. C. Bento,<sup>1</sup> and M. L. Baesso<sup>1,\*</sup>

<sup>1</sup>*Departamento de Física, Universidade Estadual de Maringá, Avenida Colombo 5790, 87020-900 Maringá, PR, Brazil*

<sup>2</sup>*Instituto de Física Gleb Wataghin, Universidade Estadual de Campinas, Unicamp, 13081 Campinas, SP, Brazil*

(Received 22 September 1999)

This work demonstrates the occurrence of  $dn/dT$  inversion from negative to positive near the nematic-isotropic phase transition in a lyotropic liquid crystal. It is suggested that this effect can be attributed to a sudden increase of the electronic polarizability due to a change in the micelle shape near this phase transition. Formation of a long lasting lenslike element within the sample when it is irradiated at moderately high laser powers is also reported. This permanent lens is erasable by increasing the temperature above the nematic-isotropic transition temperature.

PACS number(s): 61.30.-v, 42.65.Jx, 64.70.Md

### I. INTRODUCTION

The similarity between lyotropic liquid crystals and biological membranes combined with the well known unique flow phenomena presented by liquid crystalline materials have attracted the attention of many researchers in the last few years. The structure of these materials consists of micelles while thermotropic liquid crystals have molecules as their unit cell. The micelles are composed of amphiphilic molecules having a hydrophilic head and a hydrophobic tail immersed in aqueous solution. The study of this class of liquid crystals is of considerable interest due to the relative lack of detailed knowledge of their physical properties as compared to the thermotropic liquid crystals, as well as to the eventual possibility for exploring these materials as sensing device elements.

Laser induced refractive index change has been widely employed in order to understand the fundamental properties of thermotropic liquid crystals [1–7]. As a result of the sample-laser beam interaction several nonlinear processes are straightforwardly induced, depending on both the liquid crystal composition and spatial orientation. Among these, the Kerr effect, electrostriction, nonlinear electronic polarization, and thermal heating processes have been observed. Discrimination among these optically induced nonlinear processes has been successfully achieved by changing the beam power and polarization, the experimental configuration, and the time scale of the experiments [8]. A detailed discussion of the basic nonlinear processes and detection techniques associated with propagation of a laser beam through liquid crystals is presented in Ref. [8].

Recently, we have reported on the use of the thermal lens (TL) technique for evaluation of the thermal diffusivity anisotropy of lyotropic liquid crystals [9,10]. With proper experimental arrangement and time scale of the measurements, thermal lens methods can be applied to evaluate the thermal contribution of the refractive index change ( $dn/dT$ ) induced by the laser beam [8]. The description of the refractive index

profile created by the conversion of the absorbed energy into heat during the formation of the thermal lens takes into account the thermal and optical properties of the sample. The TL is a remote local probe technique that allows a better definition of the critical temperature at the phase transition when compared to the usual calorimetric methods. Conventional methods have shown that for thermotropic nematics the refractive index and consequently  $dn/dT$  have an unusually large temperature dependence near the nematic-isotropic phase transition [8]. This behavior has been mainly correlated with the high variation of the sample order parameter(s) occurring at this temperature range. As far as we know, the temperature dependence of these properties has not yet been reported for lyotropic liquid crystals. Our hypothesis is that these rapid and intense changes in the anisotropy of the sample properties at the phase transition can be evaluated by the TL technique, providing more information about the structural and thermo-optical responses of the system investigated. Furthermore, with the quantitative theoretical treatment already available for this method, these properties can be determined absolutely.

In this paper, we have applied the TL technique to investigate the temperature dependence of the rate of change of the refractive index in a lyotropic liquid crystal. In particular, we focus our attention on the temperature range from 48°C up to 52°C, where this material presents a nematic-isotropic phase transition ( $N \leftrightarrow I$ ).

### II. EXPERIMENT

The lyotropic liquid crystal sample was prepared with the following composition: potassium laurate (29.4 wt%), decanol (6.6 wt%), and water (64 wt%). The phase sequences were determined by optical microscopy and conoscopic observations, which showed that it was isotropic up to 15°C, calamitic nematic from 15°C to 50°C, and isotropic again above 50°C. The width of the nematic-isotropic phase transition of this sample is approximately 1°C. The sample was placed in a quartz cuvette 0.5 mm thick. After remaining 15 h in a magnetic field (1.5 T) the director was aligned in parallel with or perpendicular to the side walls. After that, the sample was positioned inside a hot stage (MK200) de-

\*Electronic address: mlbaesso@dfi.uem.br

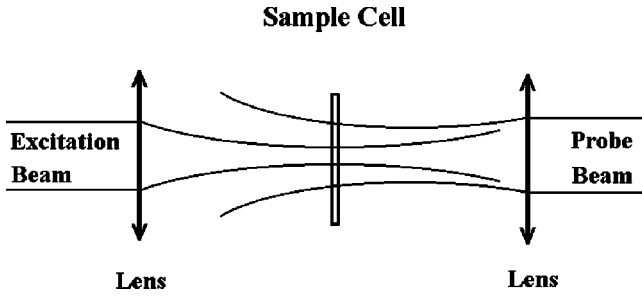


FIG. 1. Probe beam and excitation beam in the mode mismatched TL configuration.

vice. For each orientation of the directors the measurements were performed as a function of the temperature in the range from 25 °C up to 54 °C. The resolution of the hot stage MK200 is 0.01 °C. The measurements were performed only when the temperature of the sample was stabilized to better than 0.1 °C.

The thermal lens experiments were performed using the mode mismatched configuration as a function of the temperature. In this arrangement the probe beam spot size is larger than the excitation beam (Fig. 1), improving the sensitivity of the technique when compared to the mode matched or single beam configuration [11,12]. An argon ion laser was used as the excitation beam (514.5 nm) and a He-Ne laser (632.8 nm) as the probe beam. The exposure of the sample to the excitation beam was controlled by a shutter. The output of the photodiode was fed into a digital oscilloscope which was triggered by a second photodiode. The data were transferred through a general purpose interface board 488.2, interface, and stored in a microcomputer for further analysis. Each scan resulted in 1000 measured points.

### III. THERMAL LENS BACKGROUND

The thermal lens effect is created when an excitation laser beam passes through the sample and the absorbed energy is converted into heat, changing the refractive index and therefore producing a lenslike optical element within the sample. The propagation of the probe beam laser through the TL results in either a defocusing ( $dn/dT < 0$ ) or a focusing ( $dn/dT > 0$ ) of the beam center. The theoretical treatment of the TL effect considers the aberration of the thermal lens as an optical path length change to the probe laser beam, which can be expressed as an additional phase shift on the probe beam wave front after its passing through the sample. The analytical expression for absolute determination of the thermo-optical properties of the sample is given by [11,12]

$$I(t) = I(0) \left[ 1 - \frac{\theta}{2} \arctan \left( \frac{2mv}{[(1+2m)^2 + v^2]t_c/2t + 1 + 2m + v^2} \right) \right]^2, \quad (1)$$

where

$$\theta = - \frac{P_e A_e l_0}{K \lambda_p} \left( \frac{dn}{dT} \right)_p, \quad v = \frac{Z_1}{Z_c}, \quad m = \left( \frac{\omega_p}{\omega_e} \right)^2. \quad (2)$$

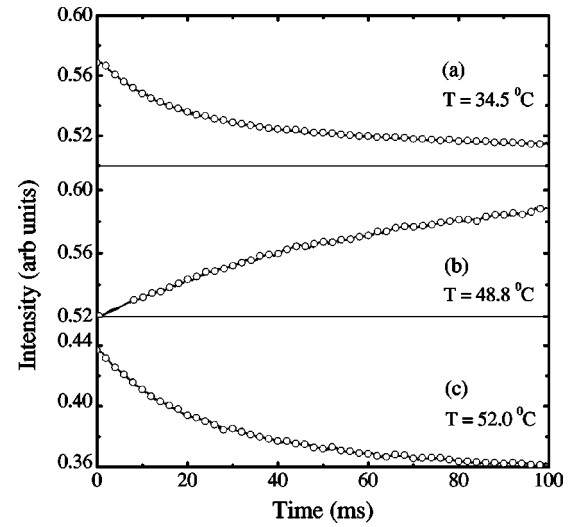


FIG. 2. TL experimental data and their best fit curve. (a) nematic phase; (b) near  $T_{NI}$ ; (c) isotropic phase.

In Eqs. (1) and (2),  $I(t)$  is the temporal dependence of the probe laser beam at the detector,  $I(0)$  is the initial value of  $I(t)$ ,  $\theta$  is the thermally induced phase shift of the probe beam after its passing through the sample,  $\omega_p$  and  $\omega_e$  are the probe beam and excitation beam spot sizes at the sample, respectively,  $P_e$  is the excitation laser beam power (mW),  $A_e$  is the optical absorption coefficient at the excitation beam wavelength ( $\text{cm}^{-1}$ ),  $Z_c$  is the confocal distance of the probe beam,  $Z_1$  is the distance from the probe beam waist to the sample,  $l_0$  is the sample thickness,  $K$  is the thermal conductivity,  $\lambda_p$  is the probe beam wavelength,  $t_c$  is the characteristic thermal lens time constant, and  $(dn/dT)_p$  is the temperature coefficient of the sample refractive index at the probe beam wavelength. In time resolved TL measurements,  $\theta$  and  $t_c$  are straightforwardly obtained from the fitting of the experimentally observed time profile of the developing thermal lens to Eq. (1). It should be noted that the above theoretical model was developed for an isotropic medium, while in the present experiments, especially in the case of the planar geometry, the parameter  $\theta$  has an effective value, defined as  $\theta_{\parallel e}$ . For homeotropic alignment there is a radial symmetry in the thermal lens profile, which means that the values of the measured parameters are related to the perpendicular orientation of the director. Here we denote  $\theta$  as  $\theta_{\perp}$ .

### IV. RESULTS AND DISCUSSION

Figure 2 shows the typical time resolved thermal lens signal for the director aligned parallel to the side walls for three different temperatures. An inversion is observed in the buildup of the thermal lens at 48.8 °C [Fig. 2(b)]. The corresponding values of  $\theta_{\parallel e}$  and  $\theta_{\perp}$  (normalized to the laser power) obtained from the phase shift signal data fitting to Eq. (1) are plotted in Figs. 3(a) and 3(b), respectively, as a function of temperature. The data points in the isotropic phase in Fig. 3(a) and Fig. 3(b) are represented by crosses. They were obtained through averaging the data from all measurements performed in this region. For the planar geometry the value of  $\theta_{\parallel e}$  decreases from about 2 at 34 °C to 0.04 at 48.3 °C and becomes negative between 48.5 °C and 49.3 °C, returning to

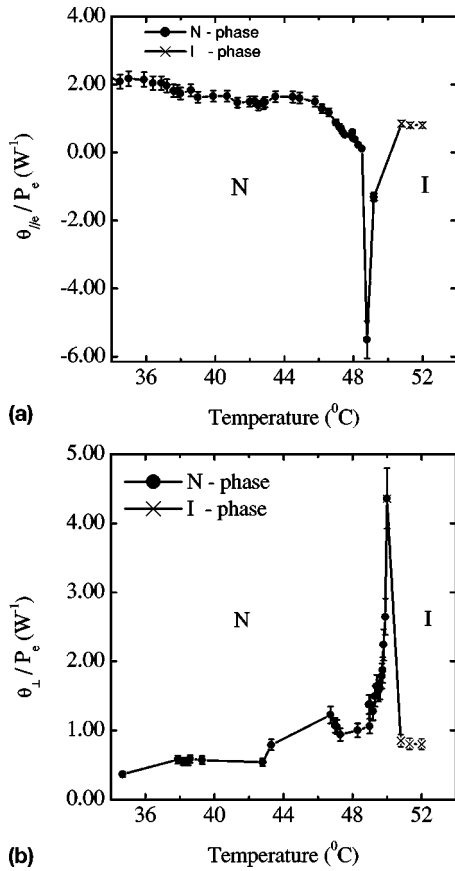


FIG. 3. (a) Normalized probe beam phase shift  $\theta_{\parallel}/P_e$ . Crosses ( $\times$ ) represent  $\theta/P_e$  in the isotropic phase. (b) Normalized probe beam phase shift  $\theta_{\perp}/P_e$ . Crosses ( $\times$ ) represent  $\theta/P_e$  in the isotropic phase.

a positive value above 49.3 °C.

It follows from Eq. (2) that this inversion of the  $\theta_{\parallel}$  sign is a consequence of a change in  $dn/dT$  from negative to positive. We note that this defocusing–self-focusing inversion was only observed for the planar geometry near the nematic–isotropic phase transition. We attribute this inversion to the rate of change of the refractive index with respect to the temperature, namely,  $dn/dT$ . First, both the probe beam and the excitation beam were perpendicularly oriented to the sample cell, therefore preventing reorientation of the director. Secondly, the probe beam polarization was parallel to the director orientation, while the pump laser beam was circularly polarized. Finally, the higher diameter of the probe beam as compared to the excitation beam seems to be a more convenient configuration for  $dn/dT$  to dominate the optical path ( $nl_0$ ) change with temperature.  $dn/dT$  can be expressed as proportional to  $A(\varphi - \beta)$  [13,14], where  $\varphi$  is the temperature coefficient of the electronic polarizability,  $\beta$  is the thermal expansion coefficient, and  $A$  is a constant that depends on the sample refractive index. In this relation  $\varphi$  and  $\beta$  are counteracting factors affecting  $dn/dT$ . In our results for the planar geometry, although the polarizability is comprised of two contributions of the refractive index change, parallel and perpendicular to the director, its value in the long axis orientation is dominant and probably controls the effective value of the probe beam phase shift  $\theta_{\parallel}$ .

Therefore, a possible mechanism driving the observed in-

version of  $dn/dT$  in the director orientation is the increase in the  $\varphi$  values in the long axis of the micelles, resulting from their higher electronic polarizability near the nematic–isotropic phase transition as compared to the nematic and isotropic phases. This agrees with the observation that in the nematic–isotropic phase transition the electronic polarizability is greatly enhanced on the axis parallel to the director [15]. The  $\varphi$  value is associated with the electronic polarizing power  $Z/a^2$ , where  $a$  is the distance between the dipole charges ( $Z$ ). A decrease in the ratio  $Z/a^2$  means a decrease in the atomic group size, producing a consequent increase in the value of these polarizing groups. This, in turn, suggests that the observed inversion in  $dn/dT$  results from a change in the micelle shape, decreasing the distance between the dipole charges. In other words, the inversion in  $dn/dT$  reveals, from a microscopic point of view, a significant change in the spatial distribution of the charges in the sample induced by a modification in its basic units. This explanation is consistent with published x-ray diffraction measurements, showing a micelle shape change near the nematic–discotic–isotropic phase transition in a lyotropic liquid crystal [16].

For the homeotropic configuration the  $\theta_{\perp}$  values increase with increasing temperature, presenting a peak at 50 °C. In this sample alignment the thermal expansion coefficient  $\beta$  dominates the observed change in  $dn/dT$ , which is negative in the whole temperature range investigated in this work.

We note that the temperature of the peak of  $\theta_{\parallel}$  for the planar alignment is smaller than that of the peak in Fig. 3(b) for the homeotropic geometry. This difference may be attributed to the fact that the electronic polarizability increases as the temperature value approaches the nematic–isotropic phase transition, overcoming the possible changes in the thermal expansion values. After reaching the minimum at about 48.8 °C,  $\theta_{\parallel}$  moves into a region where its values increase until reaching the isotropic phase, indicating that in this temperature range the thermal expansion coefficient increases and dominates  $dn/dT$ . For the homeotropic geometry, as mentioned before, the thermal expansion coefficient dominates  $dn/dT$  in the whole temperature range and becomes maximum just before the isotropic phase. The above results indicate that thermal lens measurements provide an alternative route for investigating the temperature dependence of  $dn/dT$ , with the advantage of allowing the measurements to be independently performed for each orientation of the director.

We next performed a second set of experiments using the same mode mismatched thermal lens experimental setup, except that the two laser beams were used with the polarization parallel to the director orientation and the probe beam profile was projected on a screen. The sample was oriented in the planar geometry at a temperature close to the phase transition. The excitation beam power was increased up to 300 mW, when a permanent lens was induced, remaining unchanged during the one hour time of observation. We found that this process could be erased by increasing the sample temperature up to the isotropic phase. We also noted that the permanent lens was greatly enhanced when the sample was doped with ferrofluid. A picture of this permanent lens is shown in Fig. 4. This memory effect is similar to the one observed by Khan [17] and Khoo and Normandin [18] in thermotropic liquid crystals and can be explained in a similar

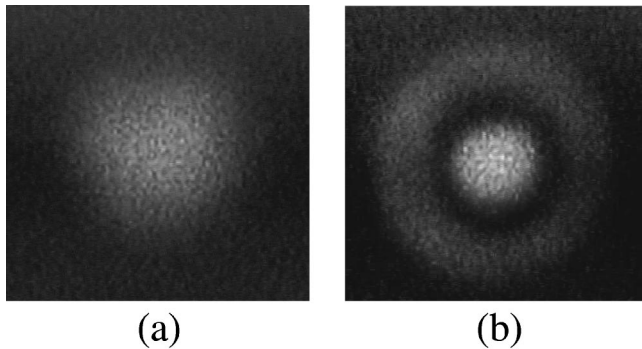


FIG. 4. (a) Probe beam pattern; (b) the observed permanent lens. The ferrofluid concentration is 0.080 wt.%.

way. The liquid crystal in the region where the excitation laser beam passes is superheated through the nematic to the isotropic phase. After the interruption of the illumination, the micelles are cooled down, remaining in a disordered state surrounded by those that were outside the laser spot and are in the ordered phase. This hypothesis was further tested by performing the TL experiment with a reduced beam power, observing a negative  $dn/dT$ . Our data have shown that in this temperature range the planar geometry provides a positive  $dn/dT$ . The negative  $dn/dT$  value observed in the center of the permanent lens suggests a nonoriented phase of the liquid crystal in this region.

In conclusion, in this paper we have reported the observation of two important effects taking place near the nematic-isotropic phase transition in lyotropic liquid crystals, previously oriented in a magnetic field. We have shown a refractive index change inversion from negative to positive and the formation of a permanent lens. The first effect was associated with a change in the micelle shape due to their higher electronic polarizability at this temperature range. As far as we know this is the first time that this effect was observed near the phase transition in lyotropic liquid crystals. Furthermore, we have noticed that the intensity of the memory effect was greatly enhanced when the sample was doped with ferrofluid. These results suggest that the TL technique in mode mismatched configuration is indeed a very useful tool for investigating quantitatively the thermo-optical properties of anisotropy of liquid crystals, specially in the temperature range where a phase transition occurs.

We hope these results may stimulate further investigation toward the detailed understanding of these phenomena, specially for the interesting biological applications one may envisage in systems exhibiting physical behavior similar to the lyotropic liquid crystals.

#### ACKNOWLEDGMENTS

We are thankful to the Brazilian Agencies CAPES, CNPq, and FAPESP for financial support of this work. The contributions of Professor L. C. M. Miranda and Professor L. R. Evangelista are also gratefully acknowledged.

- 
- [1] I.C. Khoo, S.L. Zhuang, and S. Shepard, *Appl. Phys. Lett.* **39**, 937 (1981).
  - [2] I.C. Khoo, *Phys. Rev. Lett.* **64**, 2273 (1990).
  - [3] I. Jánossy, *Phys. Rev. E* **49**, 2957 (1994).
  - [4] D. Paparo, L. Marruci, G. Abbate, and E. Santamato, *Phys. Rev. Lett.* **78**, 38 (1997).
  - [5] R. Muenster, M. Jarasch, X. Zuang, and Y.R. Shen, *Phys. Rev. Lett.* **78**, 42 (1997).
  - [6] H.J. Eichler, G. Holliger, R. Macdonald, and P. Meindel, *Phys. Rev. Lett.* **78**, 4753 (1997).
  - [7] Y.G. Fuh, and R.F. Code, *Can. J. Phys.* **62**, 40 (1984).
  - [8] I. C. Khoo and S. T. Wu, *Optics and Nonlinear Optics of Liquid Crystals* (World Scientific Singapore, 1993).
  - [9] A.C. Bento, A.J. Palangana, L.R. Evangelista, M.L. Baesso, J.R.D. Pereira, E.C. da Silva, and A.M. Mansanares, *Appl. Phys. Lett.* **68**, 3371 (1996).
  - [10] M.L. Baesso, J.R.D. Pereira, A.J. Palangana, A.C. Bento, L.R. Evangelista, and A.M. Mansanares, *Braz. J. Phys.* **28**, 359 (1998).
  - [11] J. Shen, R.D. Lowe, and R.D. Snook, *Chem. Phys.* **165**, 385 (1992).
  - [12] J. Shen, M.L. Baesso, and R.D. Snook, *J. Appl. Phys.* **75**, 3738 (1994).
  - [13] M.L. Baesso, J. Shen, and R.D. Snook, *J. Appl. Phys.* **165**, 3732 (1994).
  - [14] L. Prod'homme, *Phys. Chem. Glasses* **1**, 119 (1960).
  - [15] G. Vertogen and W. H. de Jeu, *Thermotropic Liquid Crystals* (Springer-Verlag, Berlin, 1988); G. Ayton and G.N. Patey, *Phys. Rev. Lett.* **76**, 239 (1996).
  - [16] Y. Galerne, A.M. Figueiredo Neto, and L. Liebét, *Phys. Rev. A* **31**, 4047 (1985).
  - [17] F.J. Khan, *Appl. Phys. Lett.* **22**, 111 (1973).
  - [18] I.C. Khoo and R. Normandin, *J. Appl. Phys.* **55**, 1416 (1984).